Synthesis and characterization of silver/silver-oxide tin film via chemical bath deposition

U. Nwankwo[a,b,*] and T. O. Daniel[a,⋆]

[a]Department of Physics, Alex Ekwueme-Federal University Ndufu-Alike Ikwo,
P.M.B 1010, Ebonyi State, Nigeria.
e-mail: udoka.nwankwo@connect.polyu.hk; daniel.thomas@funai.edu.ng
[*]url: https://orcid.org/0000-0003-1049-6831;
[⋆]url: https://orcid.org/0000-0002-5176-9181
[b]Department of Applied Physics, The Hong Kong Polytechnic University,
Hong Kong SRC, China.

The chemical bath deposition technique was used to deposit Ag/AgO films on a glass substrate using silver nitrate (AgNO3) and tri-ethanolamine (a polymer matrix) as the complexing agent. X-ray diffraction (XRD) was used to study the crystalline structure of the films, scanning electron microscopy (SEM) was used to study the micrograph/morphology, and energy dispersive spectroscopy (EDS) was used for elemental composition analysis. Four peaks at 2θ values of 38.05°C, 44.15°C, 64.31°C, and 77.41°C matched the (111), (200), (220), and (311) peaks, respectively, indicating that the obtained films were crystalline. The Ag/AgO films had a relatively low transmittance value of approximately 12% in the wavelength range of 300 to 1100 nm, a band gap energy of less than 2 eV, and a high absorbance of $\geq 80\%$, suggesting applications in photothermal, photoelectronic devices/systems, architectural coatings, and other areas where spectrally selective films are of interest.

1. Introduction

The development of functional materials often involves synthesizing novel materials to enable new applications. Nanomaterials have garnered significant interest due to their small size and potential across various industries, including biomedical and electronic fields. By reducing materials to the nanoscale, new functions and quantum effects can be achieved, particularly with semiconductor and metal nanoparticles. These advancements are notable in fields like biology and medicine, where gold nanoshells, quantum dots, and super-paramagnetic nanoparticles are used for imaging and drug delivery among others [1,2].

Silver (Ag) is valued for its exceptional properties, including electrical conductivity, antimicrobial effects, and optical capabilities, making it superior to other metals. Its low toxicity allows for use in disinfectants, drug delivery, and textiles. Silver oxide exists in multiple phases: AgO, Ag_2O, Ag_2O_3, and Ag_3O_4, each with unique optical and electrical properties. These oxides are utilized in photocatalysis, photovoltaic applications, energy storage, and flexible electronics. Methods such as thermal oxidation, electron beam evaporation, and chemical vapor deposition are commonly used to grow silver oxide thin films [3–6].

Recent literature highlights the successful preparation of silver nanoparticles within bacterial cellulose membranes using triethanolamine (TEA) as a stabilizer and reducing agent. This approach yields well-dispersed spherical particles, with TEA's low content resulting in a mix of silver and silver oxides [7].
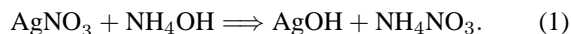
This study, "Synthesis and Characterization of Silver/Silver Oxide Thin Film via Chemical Bath Deposition (CBD)" presents a unique and economical technique for employing CBD to create homogeneous Silver/Silver Oxide thin films. It draws attention to the novel pairing of silver and silver oxide in a single film, which exhibits encouraging qualities for use in photovoltaics, sensors, and catalysis, among other fields. In addition, the study offers a thorough examination of the thin films' optical and structural qualities, connecting synthesis parameters to material attributes. In comparison with earlier studies, this work provides an examination of the structural and optical properties, demonstrates how synthesis parameters directly affect material performance, and offers substantial improvements in the uniformity and control of the film properties.

Chemical bath deposited Silver/silver oxide thin films are expected to demonstrate superior optical and structural properties relative to those deposited by alternative methods. The synthesis parameters of CBD, including temperature, pH, and reactant concentrations, will have a significant impact on the morphology, crystallinity, and optical absorption of these thin films. In addition, silver and oxides are expected to be mixed with a single film at the same time to improve the performance in device applications.
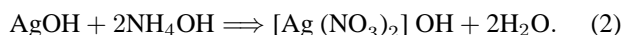
2. Experimental procedure

Soda lime glass substrates were immersed into dilute hydrochloride acid (HCl) for 24 hours after which the substrates were washed with distilled water and then dried in air to ensure good adhesion and uniformity of films onto the substrate. A 100 ml beaker was employed as bath container with a synthetic foam cover which serve not only to protect the reaction baths from dust and other environmental impurities, but also to suspend the substrates in such a way as not to touch the bottom or wall of the bath container. The reaction baths were thoroughly stirred using magnetic stirrer; in that it gives uniform and homogeneous stir. The thermometer aided in maintaining the temperature of the baths and was regulated by turning off or on the heater when the temperature was about to exceed or fall below the range of 40-55°C. Triethanolamine (TEA) was added slowly to 0.001 M of $AgNO_3$ in 100 ml beaker using a syringe until 2 ml of it was dropped in each beater while the baths were under constant stirring on a magnetic stirrer with distilled water added to make a total volume of 80ml in each bath. Four pre-treated glass substrates carefully suspended from synthetic foam covers were immersed vertically in each of the bath solutions. The baths were kept at 40-55°C on an electric heater. The first two substrates were removed one from each bath at about 60 minutes, washed with distilled water and dried in air. Subsequent ones were removes at an interval of 25 minutes; each washed and dried in air after which the samples were taken for characterization. The experimental set up is shown in Fig. 1 while Table I shows the time of synthesis of Ag/AgO thin film, the volume of TEA used, the molarities of $AgNO_3$ and the total volume of the bath solutions.

It is known that silver ions can be complexed by ammonium hydroxide according to the following reactions:

$$AgNO_3 + NH_4OH \Longrightarrow AgOH + NH_4NO_3. \quad (1)$$

In excess of NH_4OH,

$$AgOH + 2NH_4OH \Longrightarrow [Ag\,(NO_3)_2]\,OH + 2H_2O. \quad (2)$$

The complexing reaction of silver ions with TEA follows a similar pathway [8].

$$AgNO_3 + [TEA]\,OH \Longrightarrow AgOH + [TEAH]\,NO_3, \quad (3)$$

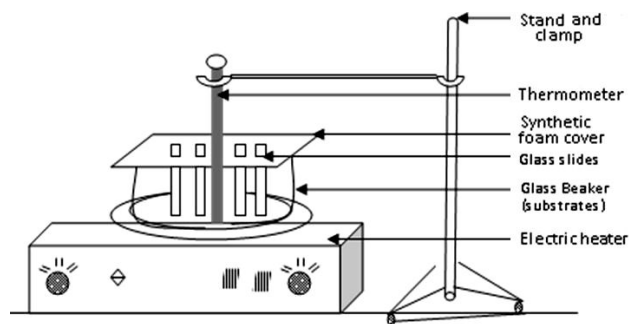$$AgNO_3 + [TEAH]\,OH \Longrightarrow [Ag\,(TEA)_2]\,OH + 2H_2O. \quad (4)$$

FIGURE 1. Skeletal representation of the experimental set-up for the synthesis of Ag/AgO thin films.

This suggests that silver nitride undergoes decomposition and depending on the experimental conditions and amount of reagent, either Ag and AgO or possible mixture of AgO, Ag_2O and higher oxides are deposition onto the substrate. However, the final product depends on the amount of TEA in solution. If enough TEA is added to completely dissolve the previously formed precipitate of AgOH, *i.e.* Ag_2O, and then an Ag film is deposited onto the substrate. Just couples of drops less of TEA produced a film of AgO onto the substrate.

3. Results and discussion

3.1. Physical appearance

A colour change of $AgNO_3$ was observed, from a colourless solution to a brownish solution, which became clear under constant stirring upon the addition of TEA, attributable to the dissolution of the initially formed precipitate. The deposited films were opaque, and the opacity increased as the deposition time increased. Although, in each case, there was uniformity and homogeneity in the dispersion of the film on the substrate, indicating that the thickness of the thin film deposits increased with time, culminating in a more reflective surface. The opacity of the film and the reflective surface were at maximum when excess TEA was added solution.

3.2. X-ray diffractometer

The X-ray diffraction spectra of the as-deposited Ag/AgO thin films are presented in Fig. 2 with 2θ values varying from 20°C to 80°C and Cu-kα radiations of wavelength $\lambda \approx 1.5406$ Å.

The appearance of Bragg peaks: 38.05°C, 44.15°C, 64.31°C, and 77.41°C were correlated with standard JCPDS-ICDD diffraction patterns from PDF-2 sets 1-43 database and there exists conformity which corresponds to the preferred orientation planes of (111), (200), (220) and (311) respectively confirming the presence of Ag/AgO films. Following the inverse law relationship of full width at half maximum β

TABLE I. Deposition parameters of Ag/AgO thin film.

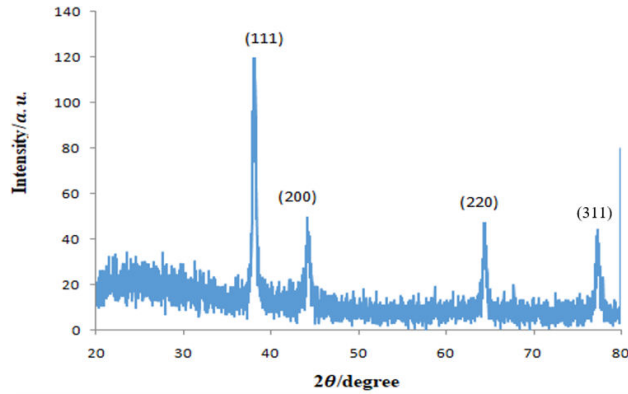| Time of Deposition (hour)	Volume of TEA (ml)	Molarities of AgNO₃ (M)	Vol. of bath solution (ml)
1.00	2.0	0.001	80.0
1.25	2.0	0.001	80.0
1.50	2.0	0.001	80.0
1.75	2.0	0.001	80.0

FIGURE 2. X-Ray diffraction pattern of Ag/AgO-TEA film.

(FWHM); Eq. (5) was used to deduce the average crystallite size which was valued as 0.21 nm after calculation.

$$D = \frac{0.9\lambda}{\beta \cos\theta}, \tag{5}$$

where λ is Cu-kα radiation wavelength (1.5406 Å), β is full width at half maximum (FWHM) in radian, θ is the Bragg angle. Using the Bragg's equation of Eq. (6), the interplanar spacing d_{hkl} was established to be averagely 1.7698Å for the grown Ag/AgO thin film.

$$D_{hkl} = \frac{n\lambda}{2\sin\theta} = \frac{a}{\sqrt{h^2 + k^2 + l^2}}, \tag{6}$$

where n corresponds to the order of the fringes and equals 1 for a special case. Other crystallographic parameters determined were macrostrain, ϵ and dislocation density, ρ given by Eqs. (7) and (8) respectively. The interplanar spacing and the macrostrain decreases as the 2θ value increases.

$$\epsilon = \frac{\beta \cot\theta}{4}, \tag{7}$$

$$\rho = \frac{15\epsilon}{aD}. \tag{8}$$

Equation (8) was established by Williamson and Smallman; where a is the lattice constant and D is the particle size. Table II shows the values calculated for as-deposited Ag/AgO thin film at the temperature range of 40° to 55°.

These parameters in Table II, contribute to the film's enhanced optical and electronic properties. The small particle size suggests high surface area and quantum effects, beneficial for applications in sensors and catalysis. The moderate dislocation density implies the presence of crystalline de-

TABLE II. Summary of structural parameters of as-deposited Ag/AgO thin film.

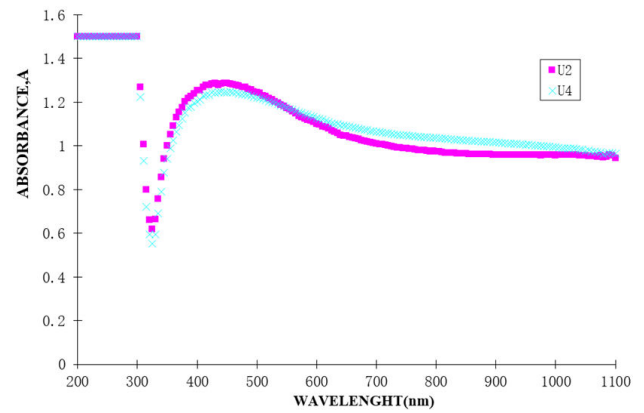| Bath temp. (°C)	Particle size (nm)	Dislocation density, ρ(Å^{-1})	Micro-strain, ϵ	Inter- planar spacing, d_{hkl} (Å)
40-55	0.2	0.65	0.37	1.77

FIGURE 3. Absorption spectra of Ag/AgO thin films.

fects, potentially increasing catalytic activity, while the macrostrain indicates structural strain that could modify the film's band structure. The interplanar spacing (1.77 Å) reflects the crystallographic orientation, essential for tailoring film properties in optoelectronics [9].

3.3. Optical analysis

Figure 3 show the optical absorption spectra of Ag/AgO thin films without taking reflection and scattering into account which was measured in the wavelength range of 200-1100 nm for the as-deposited films. The Ag/AgO thin films showed a high absorbance value.

The transmittance spectra for the films is shown in Fig. 4. Despite the slight increase of transmittance through the visible spectrum, there was stability in its measurement at wavelength $\lambda \approx 1100$ nm. Thicker Ag/AgO thin-film films exhibit lower transparency, especially in the visible spectrum, according to their transmittance spectra. This is corroborated by recent studies, which show that increased thickness of silver oxide thin films reduces transmittance mainly because of increased light absorption and scattering. In the visible spectrum, for instance, films that are thicker than 100 nm have transmittance below 20%, according to Patel et al. [10]. According to Wang et al. [11], developments in chemical bath
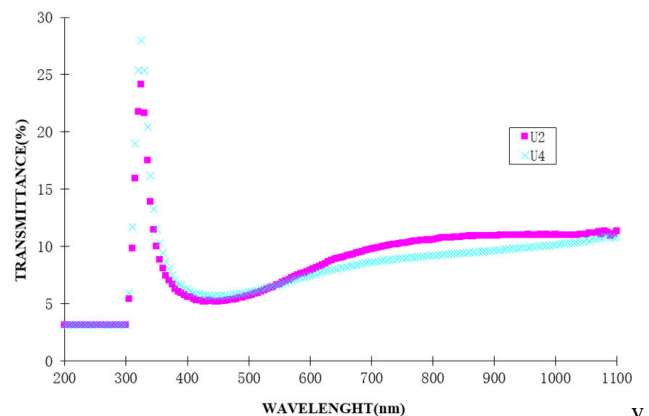

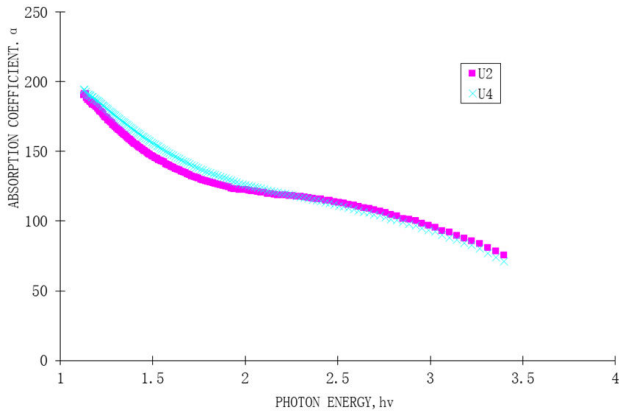FIGURE 4. The Transmittance spectra (%) for Ag/AgO thin films.

FIGURE 5. Variation of the absorption coefficient with photon energy for Ag/AgO thin films.

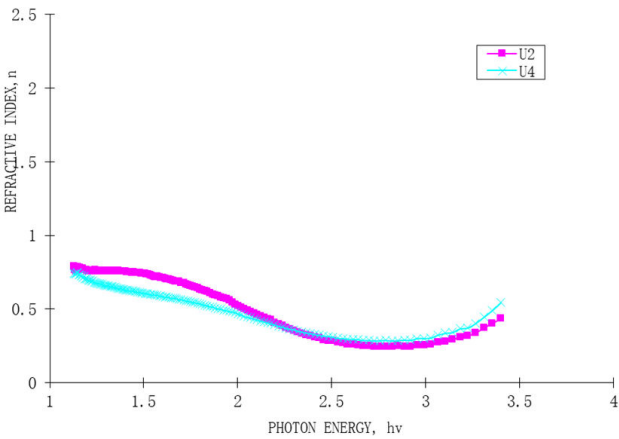FIGURE 7. Variation of $(\alpha h\nu)^2$ against hv for Ag/AgO films.

FIGURE 6. Variation of the refractive index with photon energy for Ag/AgO thin films.

deposition processes have made it possible to better control layer thickness, which has improved both transparency and electrical conductivity.

Figures 5 and 6 depicts the variation of absorption coefficient and refractive index with photon energy. The values of absorption coefficient were calculated using Eq. (9):

$$I_t = I_0 \exp \alpha t, \qquad (9)$$

where α is the absorption coefficient; t is film thickness, I_0 and I_t are the intensities of initial and transmitted light respectively.

The absorption coefficient (α) is related to the incident photon energy by:

$$\alpha = \frac{K(h\nu - E_g)^{\frac{1}{2}}}{h\nu}, \qquad (10)$$

where K is a constant, E_g is the energy band gap and n is a constant equal to 2 for direct band gap. Figure 7, shows the variation of $(\alpha h\nu)^2$ versus $h\nu$ for Ag/AgO films. The graph gave the direct band gap values, obtained by extrapolating the linear line on hv axis as 1.5 and 1.6 eV for the films.
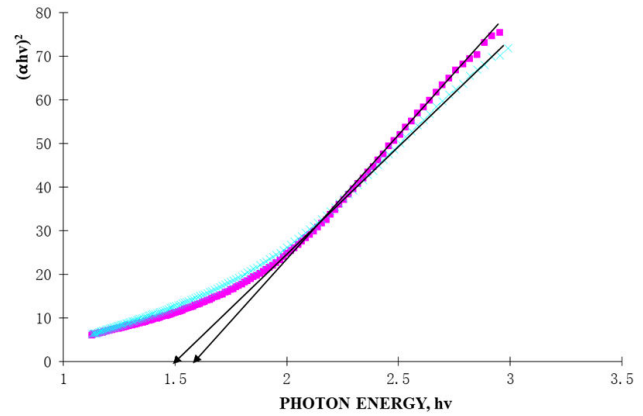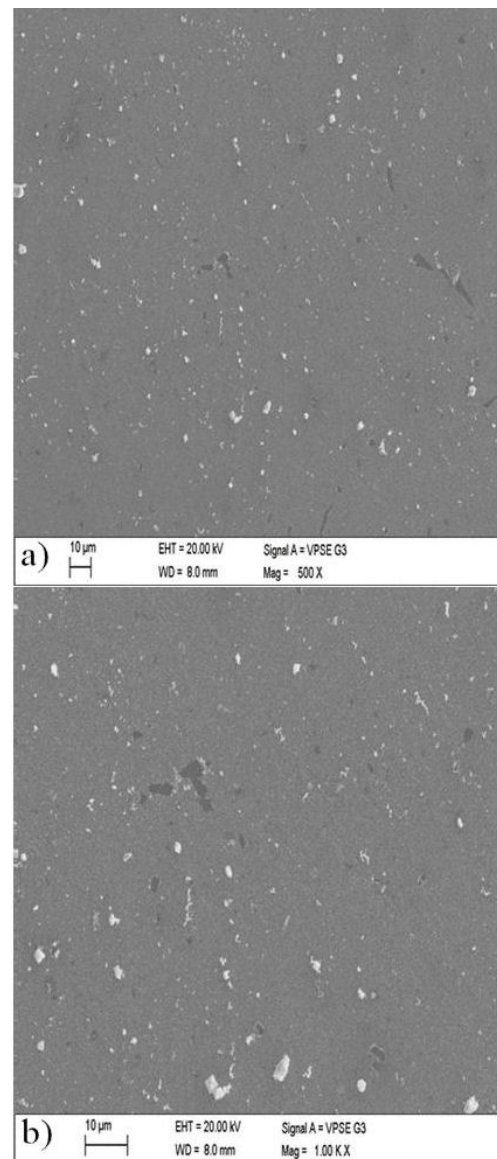

FIGURE 8. SEM images of Ag/AgO films coated on glass substrates.

3.4. Morphological analysis

The scanning electron micrographs of the Ag/AgO thin film coated on glass substrates shed light on the surface morphology of the film as shown in Fig. 8. The micrographs show a black, granular surface with different-sized and shaped grains. Notably, there are no holes or cracks evident on the surface, demonstrating the consistency and strength of the deposition. Nonetheless, the grains were uniformly dispersed, with certain regions exhibiting agglomeration. Approximately 20 μm is the average grain size, as determined by ImageJ software [12, 13]. This grain size is in line with similar research [14, 15] that highlights the impact of deposition conditions on thin film microstructure. The uneven grain distribution seen in the SEM pictures is characteristic of films deposited via chemical bath deposition (CBD), where the nucleation and development of grains are greatly influenced by bath temperature, pH, and reactant concentration, among other variables [16].

The significance of optimizing these parameters to attain the intended grain size and morphology has been brought to light by recent developments in the synthesis of Ag/AgO thin films using CBD. For example, Wang *et al.* [11] work from 2023 showed that changing the bath solution's pH may greatly lower agglomeration and enhance the uniformity of grain distribution. In a similar vein, Liu *et al.* [17] discovered that regulating the deposition temperature might improve the optical and electrical properties of Ag/AgO thin films by increasing their crystallinity and decreasing their structural defects.

3.5. Energy dispersive X-Ray analysis

The EDX spectrum in Fig. 9, recorded along the cross-section of the sample reveals the presence of Ag crystallite. The diagram shows the presence of a peak associated to the Ag ($\approx$ 22.20%) atoms. Almost disappearing peak of oxygen suggest that it is a contribution from the glass substrates giving an elemental composition of Ag/O-Si-Ca-Al-Na-Mg-S. Traces of these elements shows that the starting materials (TEA and AgNO3) could contain some impurities. It is not unexpected that traces of Si, Ca, Al, Na, Mg, and S were observed, as these elements are common components of the glass substrate, which contains them as active ingredients.
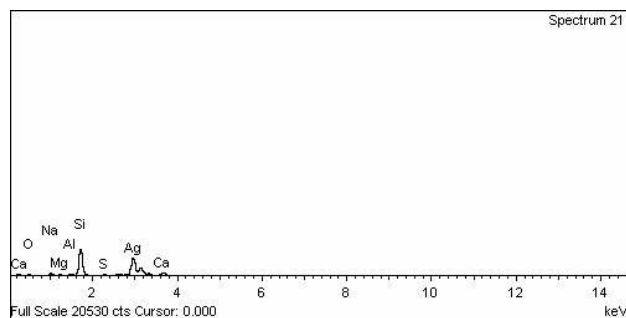

FIGURE 9. EDX spectrum of Ag/AgO.

Daniel *et al.* [18] has reported similar phenomenon for soda lime glass substrate.

4. Conclusions

Using Ag+ - triethanolamine (TEA) as the precursor, an aqueous chemical bath deposition technique was used to synthesize Silver/Silver oxide thin films at temperatures between 40 and 55 °C. This confirmed the hypothesis that CBD can produce films with better optical and structural properties than other methods. The resultant films had a poor transmittance of about 12% and a high absorbance of $\geq$80%, exhibiting uniformity and reflection. The films appear to be suited for applications requiring spectrally selective films, such as electronics, optoelectronics, photothermal, and related applications, based on their direct energy band gap ($E_g < 2$ eV). The study demonstrated how the synthesis factors affected the Ag/AgO films' morphology and optical properties. As a potent reducing agent and a silver ion chelating agent, TEA had a dual purpose in regulating nucleation, particle development, and eventually particle size. The deposition method may be fine-tuned to make films with the necessary silver oxide content by tuning TEA concentration. This would increase the films' potential for use in solar cells, thermal control window coatings, anti-reflective coatings, and other cutting-edge technical fields. These results support the hypothesis that CBD can synthesize high-performance Ag/AgO thin films for device applications by highlighting the significance of meticulously regulating the synthesis conditions to obtain the required film properties.

1. Y. J. Wang *et al.*, The use of polymer-based nanoparticles and nanostructured materials in treatment and diagnosis of cardiovascular diseases: Recent advances and emerging designs. *Progress in Polymer Science*, **57** (2016) 153-178.

2. A. G. Niculescu and A. M. Grumezescu, Polymer-based nanosystems-A versatile delivery approach. *Materials*, **14** (2021) 6812, https://doi.org/10.3390/ma14226812.

3. J. H. Zhang, S. Z. Wang, J. B. Liu, Z. L. Wang, and N. B. Ming, Preparation and absorption properties of polystyrene/Ag/TiO$_2$ multiple coated colloids. *Journal of Materials Research*, **20** (2015) 965-970.

4. K. Ma, and Z. An, Macromolecular rapid communications. *Macromolecular Rapid Communications*, **37** (2016) 1632.

5. A. Hammad, M. Abdel-Wahab, and A. Alshahrie, Structural and morphological properties of sputtered silver oxide thin films: The effect of thin film thickness. *Digest Journal of Nanomaterials and Biostructures*, **11** (2016) 1245-1252.

6. J. Kwon *et al.*, Recent progress in silver nanowire based flexible/wearable optoelectronics. *Journal of Materials Chemistry C*, **6** (2018) 7445-7461.

7. H. S. Barud *et al.*, Self-supported silver nanoparticles containing bacterial cellulose membranes. *Materials Science and Engineering: C*, **28** (2008) 515-518.

8. N. Vigneshwaran, R. P. Nachane, P. V. Vardarajan, and R. H. Balasubramanya, A novel one-pot 'green' synthesis of stable silver nanoparticles using soluble starch. *Carbohydrate Research*, **341** (2009) 2012-2018.

9. W. Sun *et al.*, SERS-active Ag-Al alloy nanoparticles with tunable surface plasmon resonance induced by laser ablation. *Optical Materials*, **96** (2019) 109298, https://doi.org/10.1016/j.optmat.2019.109298.

10. K. Kayed, The optical properties of individual silver nanoparticles in Ag/Ag$_2$O composites synthesized by oxygen plasma treatment of silver thin films. Plasmonics (2020). https://doi.org/10.1007/s11468-020-01169-9.

11. B. El-Ghmari, H. Farah, and A. Ech-Chahad, A new approach for the green biosynthesis of silver oxide nanoparticles Ag$_2$O, characterization and catalytic application. *Bulletin of Chemical Reaction Engineering & Catalysis,* **16** (2021) 651-660, https://doi.org/10.9767/bcrec.16.3.11577.651-660.

12. T. O. Daniel, U. E. Uno, K. U. Isah, and U. Ahmadu, Optimization of electrical conductivity of SnS thin film of $0.2 < t \leq 0.4$ μm thickness for field effect transistor application. *Rev. Mex. Fis.*, **67** (2021) 263-268.

13. T. O. Daniel, U. E. Uno, K. U. Isah, and U. Ahmadu, Tuning of SnS thin film conductivity on annealing in an open air environment for transistor application. *East European Journal of Physics*, **2** (2020) 94-103.

14. S. W. Balogun, A. B. Abdulhamid, Y. K. Sanusi, and O. Adedokun, Synthesis and characterization of silver nanoparticles-doped titanium (IV) oxide thin films. *IOP Conference Series: Materials Science and Engineering,* **805** (2020) 012034. https://doi.org/10.1088/1757-899X/805/1/012034.

15. R. K. Sharma, *et al.*, Silver nanomaterials: Synthesis and (electro/photo) catalytic applications. *Chemical Society Reviews*, **50** (2021) 11293, https://doi.org/10.1039/d0cs00912a.

16. M. Li, Y. Wang, Y. Xing, and J. Zhong, P123-assisted preparation of Ag/Ag$_2$O with significantly enhanced photocatalytic performance. *Solid State Sciences*, **99** (2020) 106062, https://doi.org/10.1016/j.solidstatesciences.2019.106062.

17. L. Gomathi Devi, and R. Kavitha, A review on plasmonic metal-TiO$_2$ composite for generation, trapping, storing, and dynamic vectorial transfer of photogenerated electrons across the Schottky junction in a photocatalytic system. *Applied Surface Science,* **360** (2016) 601, https://doi.org/10.1016/j.apsusc.2015.11.168.

18. T. O. Daniel, U. E. Uno, K. U. Isah, and U. Ahmadu, Electric double layer field effect transistor using SnS thin film as semiconductor channel layer and honey gate dielectric. *East European Journal of Physics*, **3** (2019) 71-80.